

ENHANCING CROP TYPE CLASSIFICATION FROM MULTI-FREQUENCY DUAL-POL SAR DATA BY PROBABILISTIC FUSION OF GAUSSIAN PROCESSES

Swarnendu Sekhar Ghosh, Sandeep Kumar, Avik Bhattacharya

Microwave Remote Sensing Lab (MRSLab)
Indian Institute of Technology Bombay
Mumbai, India

Dipankar Mandal

Department of Agronomy
Kansas State University
Manhattan, KS 66506, USA

Biplab Banerjee

Centre of Studies in Resources Engineering
Indian Institute of Technology Bombay
Mumbai, India

Narayananarao Bhogapurapu, Paul Siqueira

Microwave Remote Sensing Laboratory
University of Massachusetts
Amherst, MA, USA

ABSTRACT

This paper proposes a novel multivariate Gaussian Process Regression (GPR) approach for multi-class crop classification. We have trained and validated the proposed model utilising backscatter information from E-SAR C- and L-band dual-polarimetric data acquired during the AGRISAR 2006 campaign. Further, we use the Product of Experts (PoE) fusion strategy to combine decisions from the proposed Gaussian Process (GP) models trained and validated independently over C- and L-band data to analyze the changes in the classification performance. The synergistic C- and L-band information show an improved classification accuracy during various phenological stages of major crop types by (a) 4 to 37 % for VV-VH backscatter intensity channels and (b) 1 to 39 % for HH-HV backscatter intensity channels.

Index Terms— Crop classification, phenology, SAR, Multi-frequency, Dual-polarization, Gaussian processes, Multi-variate regression, Data fusion.

1. INTRODUCTION

Crop classification is pivotal in monitoring agricultural landscapes, aiding resource allocation, optimizing yield predictions, and promoting sustainable farming practices. Synthetic Aperture Radar (SAR) data, known for its all-weather imaging capability and sensitivity of its polarimetric measurements towards physical and scattering properties of the targets, has gained global significance in crop mapping [1]. Unlike other land cover classes, crop structures undergo dynamic changes during phenological stages, with radar backscatter influenced by crop structure, soil attributes, moisture content, surface roughness, plant density, and row orientation. Besides full-polarimetric SAR data, dual-polarimetric SAR data has been gaining attention [2] because of their

larger swath width and lower data volumes, but at the expense of polarimetric information. Presently, Sentinel-1, RADARSAT-2, RADARSAT Constellation Mission (RCM), and RISAT-1A provide uninterrupted global C-band SAR data coverage. With upcoming launches of SAR missions operating at different frequencies (L-, X-, and P- bands) like NISAR, ROSE-L, and EOS, the prospect of achieving continuous multi-frequency SAR coverage edges toward reality. Besides using single frequency information for crop classification, previous studies instantiated the importance of combining complementary information from multiple frequencies to enhance classification performance [3]. Machine learning, particularly non-parametric models, has proven effective in crop classification studies. Gaussian processes (GPs) following a Bayesian framework stand out among these non-parametric models, demonstrating flexibility in capturing complex non-linear relationships and providing probabilistic outputs. GPs have shown promising results in various earth observation applications, including biophysical parameter retrieval [4], land-cover classification [5], and crop yield prediction [6]. Although beneficial, the computational complexities associated with the posterior approximation in GPs because of the non-Gaussian likelihood in the case of classification scenarios limit their usage to high computational systems [7].

In this context, this study proposes a novel approach to multi-class crop classification using Gaussian Process Regression (GPR) to address these computational limitations. Additionally, we implement a probabilistic fusion strategy to enhance the model's performance at various phenological stages of the crops by combining the classification decisions of multiple GPs for different frequencies of SAR data.

2. STUDY AREA AND DATASET

In this present study, we have utilized backscatter intensities (a) σ_{VV}^o and σ_{VH}^o , and (b) σ_{HH}^o and σ_{HV}^o of the C_2 matrix generated from the airborne E-SAR L-band full-pol datasets. We have also utilized dual-pol data sets derived from E-SAR C-band data for model performance tests. The multi-temporal SAR data along the East-West track were acquired during the ESA-funded AGRISAR 2006 campaign between 19th of April to 2nd of August 2006 [8] over the DEMMIN (Durable Environmental Multidisciplinary Monitoring Information Network) super-site ($53^{\circ}45'40.2''$ N, $13^{\circ}27'49.45''$ E) located in Western Pomerania, northeast of Germany. The major crop types in this region are maize, sugar beet, winter barley, rapeseed and winter wheat. The phenology calendar of the major crop types has been shown in Fig. 1. Backscatter information derived from the data acquired on 19th April (DOY=109), 5th May (DOY=125), 7th June (DOY=158), 5th July (DOY=186) and 2nd August (DOY=214) have been considered as features for modelling the GP multi-class classification model.

3. METHODOLOGY

In this research, the methodology is twofold. At first, we propose a novel approach towards classification utilising a GPR strategy. Secondly, we combine classification decisions from multiple GPs using a probabilistic fusion strategy.

Classification using regression: In a classification problem, for a given set of data points $\mathbf{X} = (\mathbf{x}_1, \mathbf{x}_2, \dots, \mathbf{x}_N)^T$, where $\mathbf{X} \in \mathcal{R}^D$ and their corresponding class labels $\mathbf{C}_c = (c_1, c_2, \dots, c_c)$ the aim is to classify an unknown unlabeled data \mathbf{x}_* . It is achieved from the posterior distribution $p(C_*|\mathbf{X}, \mathbf{x}_*, \mathbf{C}_c)$, where C_* denotes the class of the unknown test data point. The covariance matrix structure of the multivariate GPR model proposed in the literature generally captures the correlation between the inputs and the outputs. We offer a multivariate GPR approach to perform classification by assuming independence across the output classes. The aim is to learn a vector-valued latent function f that relates the input variables \mathbf{X} with the target labels/classes \mathbf{Y} in the output space $\in \mathcal{R}^Q$, where Q is the number of target classes. A Gaussian process (GP) prior on the latent function $f \sim \mathcal{GP}(t(\mathbf{X}), \mathbf{Z}(\mathbf{X}, \mathbf{X}))$ is assumed whose mean vector is 0 and a positive semi-definite covariance matrix $\mathbf{Z}(\mathbf{X}, \mathbf{X})$. The structure of $\mathbf{Z}(\mathbf{X}, \mathbf{X}) \in \mathcal{R}^{NQ \times NQ}$ because of independence assumption across the output classes is a block diagonal matrix and can be expressed as,

$$\mathbf{Z} = \begin{bmatrix} \mathbf{Z}_1(\mathbf{X}, \mathbf{X}) & 0 & 0 \\ 0 & \ddots & 0 \\ 0 & 0 & \mathbf{Z}_Q(\mathbf{X}, \mathbf{X}) \end{bmatrix}$$

The diagonal elements $\mathbf{Z}_k(\mathbf{X}, \mathbf{X})$ are the covariance matrices $\in \mathcal{R}^{N \times N}$ where $k = 1, 2, \dots, Q$. As a homoscedastic

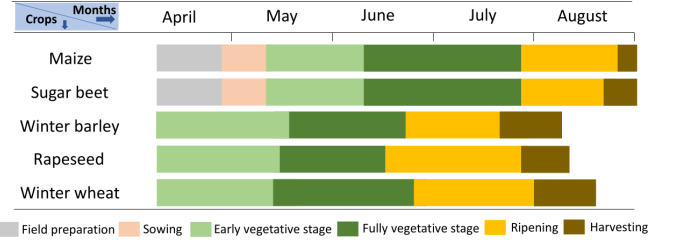


Fig. 1: Phenology stages of major crop types at DEMMIN test site.

Gaussian process model is considered so we assume an additive independent and identically distributed Gaussian noise ϵ with variance σ_n^2 ($\mathbf{Y} = f(\mathbf{X}) + \epsilon$) for modelling. Now, following a regression strategy as the prior and the likelihood remains Gaussian, the relevant integrals for the posterior approximation remain tractable and straightforward. Doing so, we overcome the challenges of a traditional GP classification approach [7]. Finally, the posterior predictive distribution for a test dataset $\mathbf{X}_* \in \mathcal{R}^{N_* \times D}$ can be expressed as,

$$p(\mathbf{f}_* | \mathbf{X}_*, \mathbf{X}, \mathbf{Y}) \sim \mathcal{N}(\mathbf{Y}_* | \widehat{\mu}_*, \Gamma_*) \quad (1)$$

where \mathbf{f}_* is the vector of functional values at test data \mathbf{X}_* , \mathbf{Y}_* is the vector of output values for test data \mathbf{X}_* , $\mathbf{Y} \in \mathcal{R}^{N \times Q}$ is the matrix of one-hot encoded output values for the observed data \mathbf{X} , $\widehat{\mu}_* \in \mathcal{R}^{N_* \times Q}$ is the vector of the means of the posterior distribution and Γ_* is the covariance matrix of the posterior distribution. The matrix $\widehat{\mu}_*$ contains the un-normalized ‘logit’ values q , the outputs of the multivariate GPR model. These logit values do not add up to 1. So, to obtain the corresponding probabilities for each class, we pass these values (q) through a Softmax function. Now, the class probabilities of the target classes add up to 1. The probabilities for $j = 1, \dots, Q$ target classes of $i = 1, \dots, N_*$ test data points, can be expressed as,

$$\sigma(q)_{ij} = \frac{e^{q_{ij}}}{\sum_{i=1}^{N_*} \sum_{j=1}^Q e^{q_{ij}}} \quad (2)$$

Hence, $\sigma(q)_{ij}$ indicates the probability value of i^{th} test data point for j^{th} class. We model separate GPs for C- and L-band. So, the resulting probability vectors for C- and L-band are expressed by,

$$\boldsymbol{\sigma}^m(q)_{ij} = [\sigma^m(q)_{i1}, \sigma^m(q)_{i2}, \dots, \sigma^m(q)_{iQ}] \quad (3)$$

where m represents the frequency C- or L-band.

Probabilistic fusion of Gaussian Processes: A probabilistic fusion strategy for synergizing decisions from the independent GPs has been developed based on the Product of Experts (PoE) approach [9]. The probability decisions from the individual GPs are utilized for each class as they are considered statistically independent. A PoE models a target probability distribution by multiplying various densities, each de-

rived from a distinct model. The resulting product is then normalized. The joint class probability from the two independent GPs can then be expressed as,

$$\sigma^{(C,L)}(q)_{ij} = \frac{\sigma^C(q)_{ij}\sigma^L(q)_{ij}}{\sum_{i=1}^{N_s} \sum_{j=1}^Q \sigma^C(q)_{ij}\sigma^L(q)_{ij}} \quad (4)$$

The joint probability vector containing the joint class probabilities can then be expressed as,

$$\boldsymbol{\sigma}^{(C,L)}(q)_{ij} = [\sigma^{(C,L)}(q)_{i1}, \sigma^{(C,L)}(q)_{i2}, \dots, \sigma^{(C,L)}(q)_{iQ}] \quad (5)$$

Consecutively, the final predicted class for an unknown test data point can be obtained by,

$$\arg \max_j \boldsymbol{\sigma}^{(C,L)}(q)_{ij} \quad (6)$$

In our study, we have undertaken a traditional pixel-based classification approach where we have utilized a stratified random sampling technique to handle the considerable class imbalance within the crop samples. The number of pixels for each crop type over the entire study area is as follows: maize (20347), sugar beet (16888), winter barley (16003), rapeseed (76079) and winter wheat (149538). It is to be noted that we have utilized < 5% of the total samples for the modelling of the Gaussian process regressor. Out of the selected samples, we considered 70% for training and 30% for testing. We assess the model's performance for multiple random training and test samples to avoid biased accuracy metrics.

4. RESULTS AND DISCUSSION

We have discussed the classification results of the proposed GP model in this section. The model's performance has been quantified in terms of Overall Accuracy (OA) and Kappa (κ) for each date. The analysis was performed independently for both C and L bands, followed by the results when synergistic information from both C- and L-bands were utilized.

(1) σ_{VV}^o & σ_{VH}^o : In the case of C-band, when the crops were at their vegetative stages, the model showed the highest accuracies between DOY-109 to DOY-158, as seen from Table 1. High misclassification within cereal crops was observed during this period, which can be attributed to their similar crop structure. As the crops progressed towards higher phenological stages, there was a decrease in the model's performance, as can be seen with the reducing overall accuracy (OA) and kappa (κ) values, because of the saturation of C-band with increasing crop biomass. In the case of the L-band, the model showed a reduced accuracy between DOY-125 and DOY-186. During the harvest stage of the crops, the increased accuracy explains their penetration capability in contrast to the C-band. When the combined information from both C- and L-band were utilized, an improvement in the model performance was observed in every stage, which highlights the

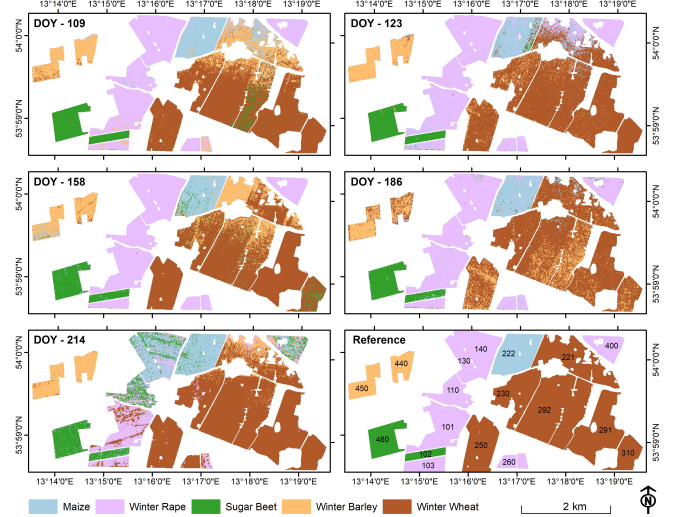


Fig. 2: Model predicted DOY wise crop classification maps over DEMMIN Site fusing dual-polarimetric (VV+VH) ESAR C- and L-band SAR data. Field Numbers have been shown in the reference map in bold.

contribution of the complementary information from both frequencies. The crop classification maps for each DOY using VV and VH backscatter intensities has been shown in Figure 2.

Table 1: σ_{VV}^o & σ_{VH}^o : Overall Accuracy (OA) and Kappa coefficient (κ) of GPC model for single-scene scenarios and when all the scenes were considered.

	DOY				
	109	125	158	186	214
C-band	OA	0.80	0.82	0.81	0.62
	κ	0.74	0.78	0.76	0.52
L-band	OA	0.84	0.81	0.73	0.73
	κ	0.79	0.77	0.66	0.66
C- and L-band	OA	0.88	0.92	0.90	0.85
	κ	0.87	0.90	0.87	0.82

(2) σ_{HH}^o & σ_{HV}^o : The performance of the GP model showed similar results in terms of OA and κ during DOY=109. However, there is a decrease in the accuracy in the case of C-band with subsequent dates, as evident in Table 2. On the other hand, the GP model shows higher accuracy across the entire phenology period for L-band as compared to the C-band. This complimentary behaviour of different bands with respect to one another can be attributed to their sensitivity towards plant morphology and also other meteorological factors. Utilising the PoE approach, the model performance enhanced when C- and L-band predictions were combined. PoE leverages the agreement between models, making the combined model more robust to individual errors and noise.

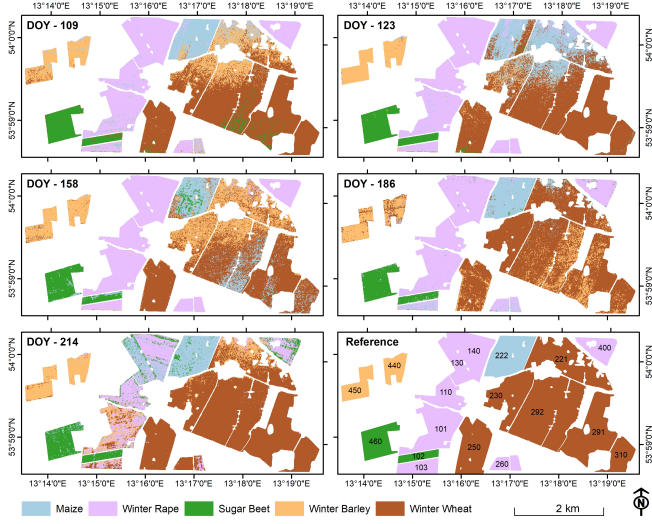


Fig. 3: Model predicted DOY wise crop classification maps over DEMMIN Site fusing dual-polarimetric (HH+HV) ESAR C- and L-band SAR data.

Also, it is simple to implement and does not require additional training or tuning parameters. Finally, the combined output remains probabilistic, which is useful for uncertainty estimation and decision-making. The crop classification maps for each DOY using HH and HV backscatter intensities has been shown in Figure 3.

Table 2: σ_{HH}^o & σ_{HV}^o : Overall Accuracy (OA) and Kappa coefficient (κ) of GPC model for single-scene scenarios and when all the scenes were considered.

		DOY				
		109	125	158	186	214
C-band	OA	0.79	0.70	0.67	0.63	0.66
	κ	0.74	0.62	0.59	0.54	0.57
L-band	OA	0.79	0.84	0.77	0.80	0.85
	κ	0.74	0.80	0.71	0.75	0.82
C- and L-band	OA	0.90	0.87	0.84	0.88	0.86
	κ	0.87	0.84	0.80	0.85	0.82

5. CONCLUSIONS

This study proposes a novel multi-variate Gaussian process (GP) regression approach to crop classification from multi-frequency dual-polarimetric SAR data to overcome the challenges of a traditional classification approach. The applicability of this method has been assessed over major crop types grown in the DEMMIN test site in Germany. Further, a probabilistic fusion strategy was formulated by integrating the decisions made by independent GPs modeled across distinct SAR frequencies. This approach aimed to boost the model's effi-

cacy during different phenological stages of the crops. Although this study presents the results of the proposed GP approach, a comprehensive analysis of the model's efficiency remains an aspect of future discussions. In addition, exploring the models capability to scale over very large datasets can be part of future analysis. With the upcoming dual-polarimetric SAR missions, implementing a Gaussian process model such as the proposed one will benefit crop classification in operational settings.

6. ACKNOWLEDGEMENT

The authors would like to acknowledge the German Aerospace Center and the European Space Agency for providing the AgriSAR 2006 campaign data through Project ID: 34188.

7. REFERENCES

- [1] D. Mandal, A. Bhattacharya, and Y. S. Rao, *Radar Remote Sensing for Crop Biophysical Parameter Estimation*, Springer, 2021.
- [2] Xiaodong Huang, Michele Reba, Alisa Coffin, Benjamin RK Runkle, Yanbo Huang, Bruce Chapman, Beth Ziniti, Sergii Skakun, Simon Kraatz, Paul Siqueira, et al., “Cropland mapping with l-band uavsar and development of nisar products,” *Remote Sensing of Environment*, vol. 253, pp. 112180, 2021.
- [3] Mario Busquier, Juan M Lopez-Sanchez, Francesca Ticconi, and Nicolas Floury, “Combination of time series of l-, c-, and x-band sar images for land cover and crop classification,” *IEEE Journal of Selected Topics in Applied Earth Observations and Remote Sensing*, vol. 15, pp. 8266–8286, 2022.
- [4] S. S. Ghosh, N. Dey, S. and Bhogapurapu, S. Homayouni, A. Bhattacharya, and H. McNairn, “Gaussian process regression model for crop biophysical parameter retrieval from multi-polarized c-band sar data,” *Remote Sensing*, vol. 14, no. 4, pp. 934, 2022.
- [5] Valentine Bellet, Mathieu Fauvel, and Jordi Inglada, “Land cover classification with gaussian processes using spatio-spectro-temporal features,” *IEEE Transactions on Geoscience and Remote Sensing*, vol. 61, pp. 1–21, 2023.
- [6] Laura Martínez-Ferrer, María Piles, and Gustau Camps-Valls, “Crop yield estimation and interpretability with gaussian processes,” *IEEE Geoscience and Remote Sensing Letters*, vol. 18, no. 12, pp. 2043–2047, 2020.
- [7] Hannes Nickisch and Carl Edward Rasmussen, “Approximations for binary gaussian process classification,” *Journal of Machine Learning Research*, vol. 9, no. Oct, pp. 2035–2078, 2008.
- [8] I. Hajnsek, R. Bianchi, M. Davidson, G. D’Urso, J. Gomez-Sánchez, A. Hausold, R. Horn, J. Howse, A. Loew, J. Lopez-Sánchez, et al., “Agrisar 2006—airborne sar and optics campaigns for an improved monitoring of agricultural processes and practices,” in *Geophys. Res. Abstr.*, 2007, vol. 9, p. 04085.
- [9] Josef Kittler, Mohamad Hatef, Robert PW Duin, and Jiri Matas, “On combining classifiers,” *IEEE transactions on pattern analysis and machine intelligence*, vol. 20, no. 3, pp. 226–239, 1998.